

gym-invmgmt: An Open Benchmarking Framework for Inventory Management Methods

Reza Barati* Qinmin Vivian Hu

Department of Computer Science
Toronto Metropolitan University, Toronto, ON, Canada

May 13, 2026

Preprint.

Abstract

Inventory-policy comparisons are often difficult to interpret because performance depends on the evaluation contract as much as on the policy itself. Differences in topology, demand regime, information access, feasibility constraints, shortage treatment, and Key Performance Indicator (KPI) definitions can change method rankings. We present **gym-invmgmt**, a Gymnasium-compatible extension of the OR-Gym inventory-management lineage for auditable cross-paradigm evaluation. The benchmark evaluates optimization, heuristic, and learned controllers under a shared CoreEnv transition, reward, action-bound, and KPI contract, while varying stress conditions through a 22-scenario core grid plus four supplemental MARL-mode rows. Within these released scenarios, informed stochastic programming provides the strongest non-oracle reference, reflecting the value of scenario hedging under forecast access, but at substantially higher online computational cost. Among learned controllers, the Proximal Policy Optimization Transformer variant (PPO-Transformer) achieves the strongest learned-policy quality at fast inference, while Residual Reinforcement Learning (Residual RL) provides competitive hybrid performance. The graph neural network variant (PPO-GNN) is highly competitive on the default divergent topology but less robust on the serial topology. Imitation learning performs well in stationary regimes but degrades under demand shift, and the bounded Large Language Model (LLM) policy-parameter baseline is best interpreted as a diagnostic controller rather than an autonomous inventory optimizer. Overall, the benchmark identifies scenario-conditioned leaders while showing that performance depends jointly on information access, demand shift, topology, and policy representation.

Keywords: *inventory management • benchmarking • reinforcement learning • operations research • graph neural networks • imitation learning • stochastic programming*

1 Introduction

Multi-echelon inventory control is difficult not only because the decision problem is stochastic and sequential (Clark and Scarf, 1960; Zipkin, 2000), but because policy performance is highly context-dependent. A replenishment rule that performs well under stationary demand, short lead times, and backlog fulfillment may fail under demand shocks, lost sales, or topology changes; similarly, a method that appears strong in one simulator may benefit from visibility, action-bound, demand-generation, or cost-accounting assumptions absent in another. Comparing policies therefore requires a shared experimental contract, not only a reported profit or service level.

Recent OR/RL benchmark efforts have moved toward such contracts: Balaji et al. (2020) introduced reusable RL benchmarks for online stochastic optimization; Hubbs et al. (2020) introduced OR-Gym, including serial multi-echelon inventory; and Perez et al. (2021) extended the OR-Gym inventory setting toward tree/network topologies while comparing deterministic linear programming, Multi-Stage Stochastic Programming (MSSP), and reinforcement learning under shared stochastic simulation mechanics. These works establish the lineage of our benchmark rather than serving as a contrast to it.

The remaining limitation is the narrowness of the comparison contract. Prior environments typically expose only part of the experimental space: stationary synthetic demand, flat observations, a fixed topology family, centralized OR/RL comparison, or decentralized multi-agent coordination. MARL benchmarks such as MABIM (Yang et al., 2023) and recent

*Corresponding author: r2barati@torontomu.ca

multi-agent supply-chain studies (Kotecha and del Rio Chanona, 2025; Quan and Liu, 2024) expand the decentralized side, but their scientific focus differs from controlled centralized cross-paradigm comparison.

Building on this lineage, we present `gym-invmgmt`,¹ a Gymnasium-compatible extension for quality–speed–robustness comparison under curated stress scenarios and explicit blind/informed information protocols. Optimization baselines use the same scenario contract, while learned policies are trained as generalist checkpoints and evaluated without scenario-specific retraining. The main study keeps centralized control as the experimental lens, isolating inventory optimization from coordination effects while retaining a per-node CTDE wrapper for decentralized diagnostics.

Contributions.

1. **Benchmark contract.** We extend the OR-Gym inventory line with configurable DAG topologies, stochastic and empirical demand, backlog/lost-sales modes, endogenous goodwill, and vector, graph, and sequence observations.
2. **Released scenario matrix.** We release 26 stress scenarios (22 core plus four MARL-mode rows) for 29 registered non-LLM configurations and one bounded LLM-policy-parameter baseline under shared action, demand, KPI, and information protocols.
3. **Generalist learned-policy evaluation.** PPO, SAC, Transformer, GNN, Residual, and imitation-learning checkpoints are evaluated without per-scenario retraining; a separate zero-shot graph-transfer stress test diagnoses cross-topology action-decoding limits.
4. **Cross-paradigm findings.** MSSP-I is the strongest non-oracle reference, information access most helps stochastic programming and variance-sensitive heuristics, and learned/LLM/transfer tests expose covariate-shift, service-level, and action-decoding limits.

2 Background and Related Work

Prior inventory-control work offers several useful but differently instrumented views of the same decision problem. The classical OR view treats inventory as a sequential decision problem, formalized by dynamic programming and Markov decision processes (Bellman, 1957; Puterman, 1994). Mathematical-programming work emphasizes planning, recourse, and safety-stock placement in networks (Graves and Willems, 2000). Replenishment-policy theory adds interpretable controls: Scarf’s min–max model is an early robust newsvendor formulation (Scarf, 1958), Zipkin systematizes inventory-policy structure (Zipkin, 2000), and Porteus develops stochastic inventory-theory foundations (Porteus, 2002). Simulation-based learning changes the lens: Giannoccaro and Pontrandolfo learn supply-chain ordering decisions through interaction (Giannoccaro and Pontrandolfo, 2002), and Kemmer et al. extend this framing in later inventory-control experiments (Kemmer et al., 2018). Subsequent deep RL studies address multi-echelon demand uncertainty (Gao and Chen, 2020), spare-parts inventory (Wang and Lin, 2021), and multi-product, lead-time-constrained networks (Meisheri et al., 2022). Data-driven inventory optimization further shows how machine-learning decision rules can move beyond purely parametric newsvendor assumptions (Ban and Rudin, 2019).

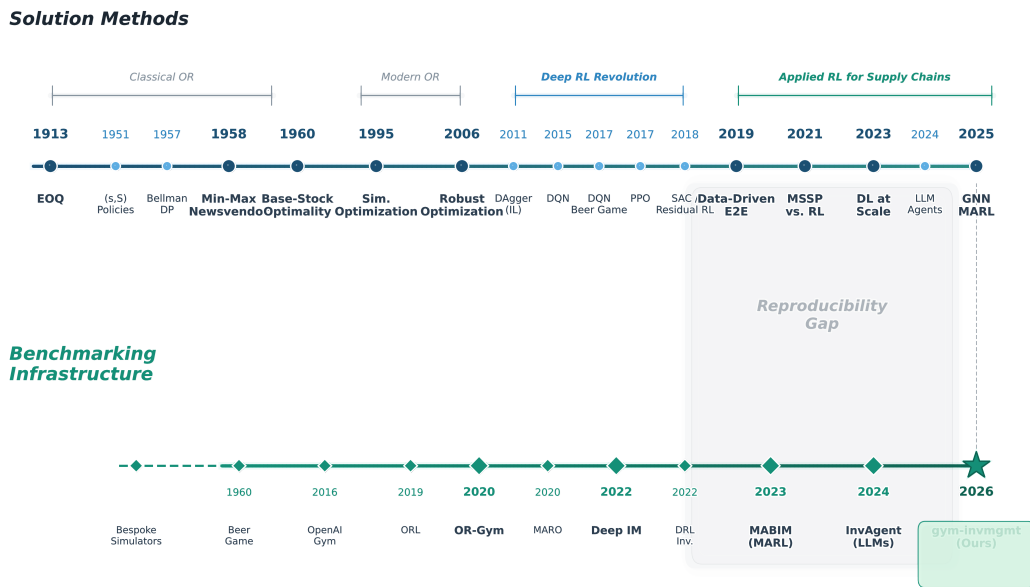


Figure 1. Inventory-method and benchmark-infrastructure timeline, from EOQ (Harris, 1913) to Gym-style OR benchmarks (Brockman et al., 2016).

¹Benchmark framework, agents, and evaluation scripts: <https://github.com/r2barati/gym-invmgmt-paper>. A standalone Gymnasium environment library covering Newsvendor, Multi-Echelon, and Network inventory problems is available separately at <https://github.com/r2barati/gym-invmgmt>.

Complementary inventory-learning studies expand important parts of this landscape: beer-game RL (Oroojlooyjadid et al., 2022), deep RL versus base-stock policies (Gijsbrechts et al., 2022), decentralized MARL benchmarks (Yang et al., 2023; Leluc et al., 2022), graph-based MARL (Kotecha and del Rio Chanona, 2025), and LLM-based inventory agents (Quan and Liu, 2024). Their focus, however, is often decentralized coordination, a specific topology, a single method family, or language-agent reasoning rather than centralized cross-paradigm evaluation under one transition, reward, action-bound, information-access, and KPI contract.

Taken together, this breadth makes numerical comparison fragile. Review and roadmap papers emphasize that DRL inventory performance depends on modeling choices, tuning burden, and evaluation design (Boute et al., 2022), and that supply-chain RL studies vary widely in formulation and assessment protocol (Rolf et al., 2023). Adjacent inventory-control studies show the same issue in other forms: centralization can change replenishment behavior (Chen and Chen, 2005), while inventory-routing formulations often embed problem-specific state, routing, and service conventions (Charaf et al., 2024). Thus, apparent performance differences may reflect the evaluation contract as much as the policy class itself.

Table 1 therefore maps representative studies along the evaluation axes needed for cross-paradigm comparison: topology, demand, action constraints, data scope, lead times, horizon protocol, observations, endogenous feedback, and evaluated algorithms. It is not a one-to-one performance comparison; it shows which parts of the experimental contract each line of work makes explicit.

Table 1. Comparison of *gym-invmgmt* to representative inventory benchmarks and studies.

Benchmark / Study	Year	Network Topology	Agent Formul.	Demand Model	Capacity/ Action Constr.	SKU & Data	Lead Times & Shortages	Horizon Protocol	Obs. Spaces	Endog. Demand Feedback	Evaluated Algorithms
ORL (Balaji et al., 2020)	2020	Single-Node	Central.	Station. Pois.	Unconstr.	1-SKU, Synth.	Fixed VLT, LS	Finite online	Flat Vec.	✗	PPO, APE-X DQN, heuristic/MIP baselines
OR-Gym (Hubbs et al., 2020)	2020	Multi-Ech.	Central.	Station. Stoch.	Prod./inv. cap.	1-SKU, Synth.	Fixed LT, BL/LS	Finite SH	Flat Vec.	✗	PPO, heuristics, MIP/SH baselines
Perez inventory (Perez et al., 2021)	2021	Multi-Ech.	Central.	Station. Stoch.	Prod./inv. cap.	1-SKU, Synth.	Het. LT, BL/LS	Finite RH/SH	Flat Vec.	✗	DLP/MSSP (RH/SH), PPO, Oracle
IM Sim. (Sridhar et al., 2021)	2021	Single-Store	Sim./Opt.	Case data	Svc. constr.	1 item, Real	Stoch. LT, LS	Finite DES	Sim. state	✗	Arena sim., OptQuest
MARLIM (Leluc et al., 2022)	2022	Single-Ech.	Decentr.	Station. ZIP	Storage cap.	50 items, Real-fit	Stoch. LT, BL/overflow	Finite episodic	Flat Vec.	✗	PPO-D/C, IPPO-C, MinMax, Oracle
Deep IM (Madeka et al., 2022)	2022	Single-Ech.	Central.	Hist./Non-Stat.	Unconstr.	Multi-SKU, Real	Stoch. VLT, LS	Historical rollout	Hist. Vec.	✗	DirectBackprop, A3C, SAC, ARS, Newsvendor
DQN Beer (Oroojlooyjadid et al., 2022)	2022	Multi-Ech.	Decentr.	Station/Step/Real	Unconstr.	1-SKU, Synth/Real	Det. LT, BL	Finite episodic	Local Hist. Vec.	✗	SRDQN, BS co-players
DRL Inv. (Gijsbrechts et al., 2022)	2022	Multi-Ech.	Central.	Station.	Feas. alloc.	1-SKU, Synth.	Fixed LT, BL/LS	Finite episodic	Flat Vec.	✗	A3C, base-stock
MengQi E2E (Qi et al., 2023)	2023	Single-Ech.	Central.	Hist./Non-Stat.	Unconstr.	Multi-SKU, Real	Stoch. VLT, LS	Finite window	Feature Vec.	✗	E2E ML, PTO, heuristics
MABIM (Yang et al., 2023)	2023	Multi-Ech.	Decentr.	Station./Non-Stat.	Warehouse cap.	2000+ SKU, Real	Var. LT, BL/overflow	Finite episodic	SKU/WH Vec.	✗	IPPO, QTRAN, BS, (s, S), hybrid BS+MARL
InvAgent (Quan and Liu, 2024)	2024	Multi-Ech.	Decentr.	Multi-Regime	Prod. cap.	1-SKU, Synth.	Fixed LT, BL	Finite episodic	Text prompt	✗	GPT-4/4o LLMs, IPPO/MAPPO, BS/tracking
GNN MARL (Kotecha and del Rio Chanona, 2025)	2025	Multi-Ech.	Decentr./CTDE	Stoch./Shock	Prod. cap.	1-SKU, Synth.	Stoch. LT, BL	Finite episodic	Network Graphs	✗	GNN-MAPPO, IPPO/MAPPO, heuristics
gym-invmgmt (Ours)	2026	Multi-Ech.	Central. (+MARL)	Stat., Non-Stat., External	Prod./action cap.	1-SKU, Synth./M5 traces	Fixed LT, BL/LS	Finite episodic/RH	Graph, Seq., Vec., Text	✓ Goodwill dyn.	Oracle, heuristics, GNN/Transformer/ST-PPO, Residual RL, Dagger/GNN-IL, LLM-Policy-C diagnostics

Note. Rows summarize each work’s primary experimental setting or released benchmark contract, not every variant studied. Endogenous demand feedback means realized service changes future demand; static stockout penalties, service constraints, and historical arrivals alone are not counted. The *gym-invmgmt* row reports the main centralized benchmark plus released diagnostic wrappers/agents. The Horizon Protocol column reports finite episodic/window evaluation and whether optimization baselines use rolling or shrinking replanning; RH/SH denote rolling/shrinking optimization horizons, while Oracle denotes a full-horizon non-causal reference. Abbrev.: Ech.=echelon; Formul.=formulation; Constr.=constraints; Obs.=observation; Endog.=endogenous; Central./Decentr.= centralized/decentralized; Stat./Non-Stat.=stationary/non-stationary; Det.= deterministic; Stoch.=stochastic; Pois.=Poisson; ZIP=zero-inflated Poisson; SKU=stock-keeping unit; Synth.=synthetic; LT/VLT=lead/vendor lead time; Het./Var.=heterogeneous/variable; BL/LS=backlog/lost sales; Unconstr.= unconstrained; Prod./inv.=production/inventory; cap.=capacity; Svc.=service-level; Feas.=feasibility-enforced; Hist.=historical; Vec./Seq.= vector/sequence; DES=discrete-event simulation; Sim.=simulation; WH=warehouse; BS=base-stock; LLM=large language model; MARL=multi-agent reinforcement learning; MIP=mixed-integer programming; PTO=predict-then-optimize; RH/SH= rolling/shrinking horizon.

3 Benchmark Framework and Environment Contract

The framework is built around a single finite-horizon environment, *CoreEnv*, defined on a directed supply-chain graph. Nodes represent production, storage, retail, or market locations; edges encode replenishment flows, retail demand links, lead times, costs, capacity/yield limits, and pipeline inventory. At each period, a controller submits a bounded reorder vector over the replenishment edges. The same transition code then applies feasibility constraints, material-balance updates, reward accounting, and KPI extraction regardless of whether the controller is an optimizer, heuristic, or learned policy.

Scenario definitions vary the experimental conditions around this shared core: topology, backlog versus lost-sales treatment, information access, demand process, external demand traces, and endogenous goodwill feedback. This separation lets the benchmark compare policy classes under matched physical mechanics rather than under method-specific state, reward, or accounting conventions.

3.1 Benchmark Scope and Information Protocol

The main benchmark adopts centralized control as a methodological lens. At each period, one controller issues replenishment requests for all reorder edges in the supply-chain graph. This choice is not a claim that real supply chains are always centrally controlled; rather, it removes decentralized coordination as a confound when comparing optimization models, heuristics, imitation learning, and neural policies under the same transition and reward contract. The per-node multi-agent wrapper is retained for diagnostic and future decentralized experiments, but the headline results use the centralized setting to isolate the inventory-control problem itself.

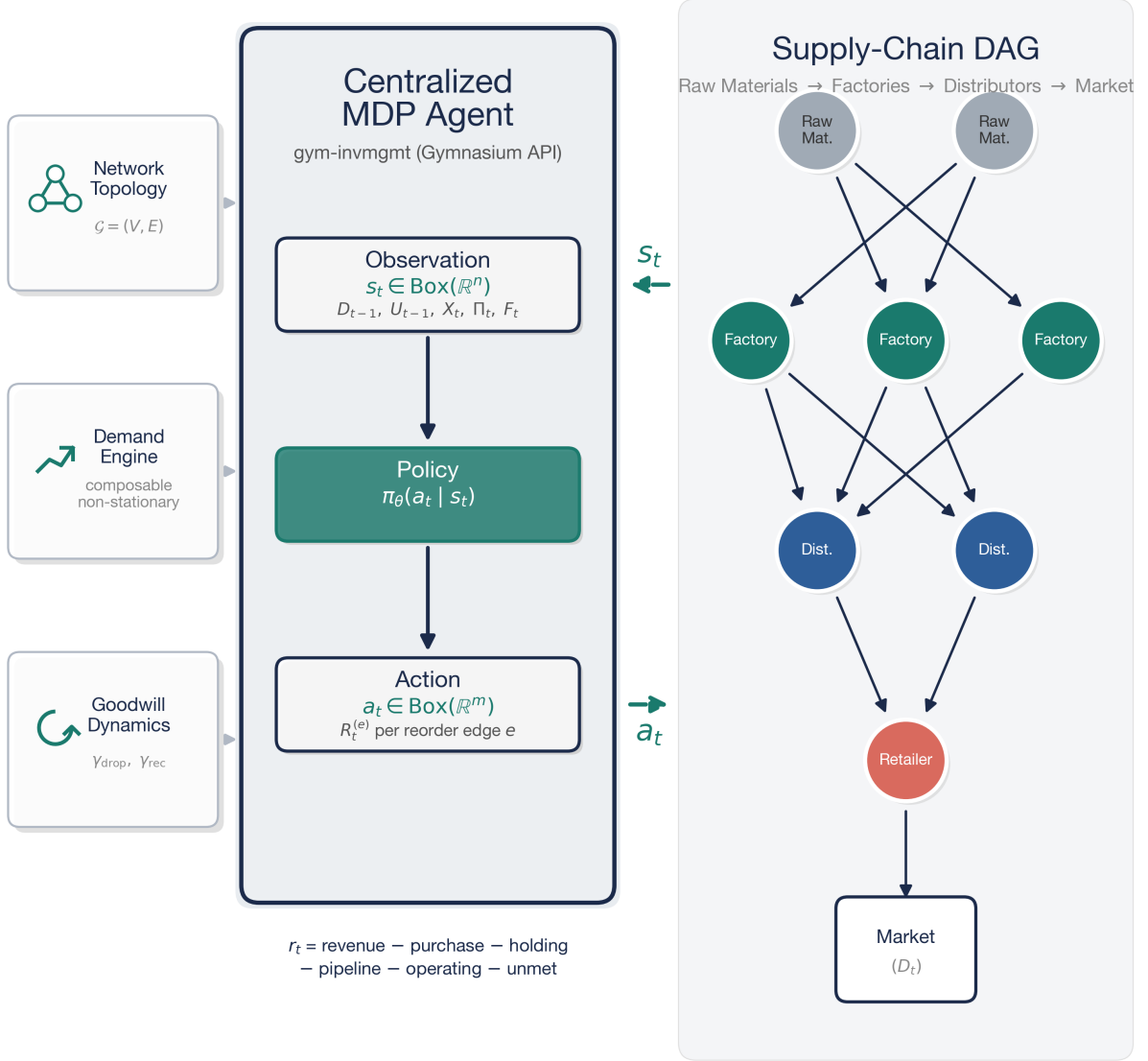


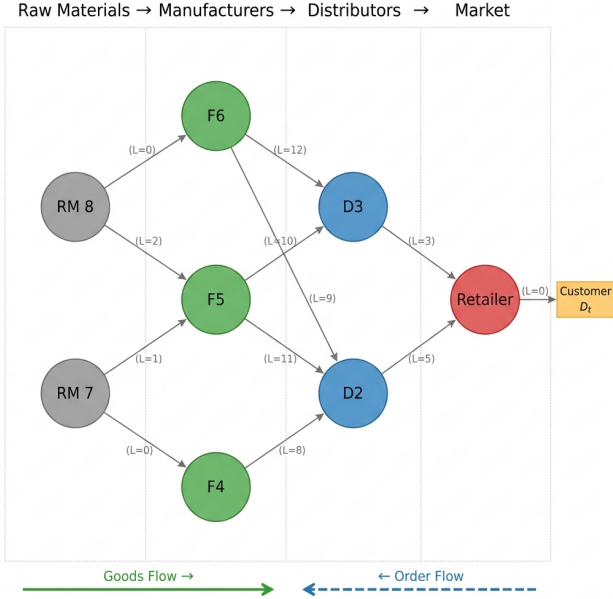
Figure 2. Schematic architecture of the `gym-invmgmt` framework. Topology, demand, and goodwill modules feed a centralized `CoreEnv Gymnasium` (Towers et al., 2023) MDP (Puterman, 1994); agents observe inventory/pipeline state and reorder on active links. Right: default divergent topology.

Information access is reported separately from policy architecture. *Blind* agents act from realized demand history, pipeline orders, and current inventory state. *Informed* agents may use benchmark demand-context features or the specified demand model, but still act causally at each decision period. The Oracle is non-causal: in exogenous-demand settings it uses future demand realizations as a full-horizon reference, while in endogenous-goodwill settings it is interpreted as a clairvoyant simulation-optimization benchmark rather than a certified dynamic-programming optimum. This separation prevents the evaluation from conflating three axes: coordination scope, demand-model access, and architectural inductive bias.

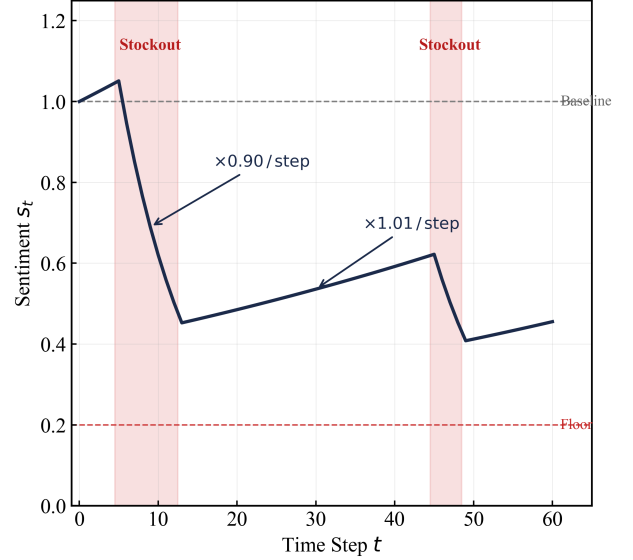
The notation follows the inventory-management MDP lineage of OR-Gym and Hubbs et al. (2020); Perez et al. (2021), while the formal finite-horizon MDP conventions follow standard stochastic dynamic programming notation (Puterman, 1994). We restate the transition and reward contract here because the benchmark extends that lineage to graph topologies, multiple observation encodings, empirical demand traces, and endogenous-goodwill stress tests. Formally, `CoreEnv` defines a graph-augmented finite-horizon MDP:

$$\mathcal{M} = (G, \mathcal{S}, \mathcal{A}, \mathcal{P}, r, \alpha) \quad (1)$$

where $G = (V, E)$ is a directed supply-chain graph, $E_r \subseteq E$ denotes the reorder edges, $\mathcal{S} \subseteq \mathbb{R}^{d_s}$ is the continuous state or wrapped observation space, and $\mathcal{A} \subseteq \mathbb{R}^{|E_r|}$ is the bounded continuous reorder space. The transition kernel $\mathcal{P}(\cdot | s_t, a_t, G)$ combines stochastic or empirical demand generation with deterministic material-balance, pipeline, feasibility, and shortage updates. The reward function r records period profit after revenue, procurement, operating, holding, shortage, pipeline, and optional fixed-ordering costs, with discount factor α .



(a) Default multi-echelon network topology (9 nodes, 12 total edges: 11 reorder links plus one retail-demand link, 4 echelons). Edge labels denote lead times (L). The legend indicates downstream goods flow and upstream order flow.



(b) Illustrative asymmetric sentiment dynamics under endogenous customer goodwill. Stockout episodes (shaded) trigger abrupt decay ($\times 0.90 / \text{step}$); recovery proceeds slowly ($\times 1.01 / \text{step}$). Floor at $S_{\min} = 0.2$.

Figure 3. (a) Default network topology used in the benchmark. Raw material suppliers feed three capacity-constrained factories, which ship through two distributors to a single retailer facing stochastic demand D_t . (b) Endogenous customer goodwill dynamics. The asymmetry between rapid sentiment decay and slow recovery rewards policies that protect service levels before stockouts compound.

Including G as a structural parameter makes topology part of the benchmark contract rather than an implicit simulator detail. Observation wrappers can expose this same physical state as flat vectors, graph features, per-link features, temporal stacks, or text prompts, allowing architecture comparisons without changing the underlying transition mechanics. All benchmark episodes remain finite-horizon simulations: learned policies act causally one period at a time, rolling-horizon OR agents repeatedly solve capped lookahead problems from the current state, and the Oracle provides the non-causal full-horizon reference where appropriate.

3.2 Graph Topologies and Observation–Action Interfaces

The framework models supply chains as Directed Acyclic Graphs (DAGs), natively defining classical serial chains and the default multi-echelon network visualized in Fig. 3a. We partition the edge set into reorder links E_r , which carry upstream replenishment requests and downstream physical shipments subject to lead times, and retail-demand links E_d , which connect retailer nodes to external markets. Topologies are parameterized procedurally or through YAML specifications, allowing researchers to define custom adjacency structures, node capacities, edge lead times, and retail demand attributes without changing the underlying transition code.

At each discrete time step t , the base environment constructs the causal observation vector

$$o_t^{\text{base}} = [D_{t-1}, U_{t-1}, X_t, \Pi_t, F_t],$$

where D_{t-1} is the last realized retail demand, U_{t-1} records previous-period unfulfilled demand (standing backlog in backlog mode and lost demand in lost-sales mode), X_t is current on-hand inventory, Π_t is an arrival-indexed pipeline schedule over reorder links, and F_t contains time and goodwill/sentiment features returned by the demand engine. The pipeline schedule is deliberately reconstructed from physically filled orders R , not raw requests a , so agents observe committed in-transit inventory rather than phantom inventory that was requested but never shipped because of upstream inventory, yield, or capacity constraints.

Observation wrappers expose this same simulator state through different interfaces. Flat-vector agents consume the base and domain-feature vectors directly; graph and per-link wrappers reshape the same state into node, edge, or link features; temporal wrappers stack recent observations for sequence policies; and text interfaces serialize selected state variables for bounded LLM-policy diagnostics. The blind/informed protocol from Section 3.1 is applied through the demand-access component of these interfaces: blind agents estimate demand context from realized history, while informed agents may use benchmark demand-context features or the specified demand model. Thus, architecture comparisons change the observation interface without changing the underlying transition mechanics.

Based on this observation, continuous replenishment actions $a_t^{(e)}$ are issued for every reorder edge $e \in E_r$. These actions represent raw replenishment requests. The environment records them for auditability, then converts them into physically filled orders $R_t^{(e)}$ after applying non-negativity, upstream inventory, yield, and capacity constraints. Neural agents are typically trained through a standard $[-1, 1]$ rescaled action interface for stable continuous-control optimization, but the shared benchmark contract evaluates all controllers through the native non-negative reorder-action space.

The resulting state vector has dimensionality $d_s = O(|V| + |E_d| + |E_r|L_{\max} + d_F)$, where L_{\max} is the longest reorder-edge lead time and d_F is the demand-engine feature dimension. This reflects node-level inventory, retail-demand and unfulfilled-demand features, and explicit pipeline tracking per reorder edge and lag period. The representation remains linear in the graph and pipeline size, while stochastic-programming scenario trees such as MSSP grow rapidly with planning horizon, branching factor, and network size (Birge and Louveaux, 2011).

3.3 Transition Dynamics and Material Balance

To ensure exactness, the environment enforces deterministic material-balance updates inside the stochastic transition kernel \mathcal{P} , following classical inventory conservation logic (Zipkin, 2000). Let $\text{pred}(j)$ and $\text{succ}(j)$ denote the immediate predecessors and successors of node j in G . Within each period, the simulator applies a fixed causal event sequence: (1) raw replenishment requests are allocated into feasible filled orders; (2) lead-time deliveries and pipeline stocks are updated; (3) goodwill is updated from the previous period's unfulfilled demand; (4) current retail demand is realized and retail fulfillment is recorded; and (5) period rewards are computed.

For each reorder edge $e = (i, j)$, the feasible filled order is

$$R_t^{(e)} = \min \left\{ \max(a_t^{(e)}, 0), \kappa_t^{(e)} \right\}, \quad (2)$$

where $\kappa_t^{(e)}$ is the link-specific feasible supply bound. External raw-material links fill any non-negative request, distributor links are capped by currently available upstream inventory, and factory links are capped by both remaining production capacity and yield-adjusted input inventory. This distinction between requested orders a_t and filled orders R_t is central to the benchmark contract.

For each managed node $j \in M$ (retailers, distributors, and factories), the on-hand inventory transition to $t+1$ is governed by:

$$X_{t+1}^{(j)} = X_t^{(j)} + \sum_{i \in \text{pred}(j)} R_{t-L_{ij}}^{(i,j)} - \frac{1}{v_j} \sum_{k \in \text{succ}(j)} S_t^{(j,k)} \quad (3)$$

where $R_\tau^{(i,j)} = 0$ for $\tau < 0$, $R_{t-L_{ij}}^{(i,j)}$ represents incoming deliveries from filled orders placed L_{ij} periods earlier, $S_t^{(j,k)}$ represents outgoing shipments fulfilled to downstream successors, and $v_j \in (0, 1]$ is the production yield factor ($v_j = 1$ for non-production nodes). Shipments are recorded in output units; a factory shipment of $S_t^{(j,k)}$ therefore consumes $S_t^{(j,k)}/v_j$ units of input inventory. Simultaneously, the in-transit pipeline inventory Y for each reorder edge $e \in E_r$ updates as:

$$Y_{t+1}^{(e)} = Y_t^{(e)} - R_{t-L_e}^{(e)} + R_t^{(e)}. \quad (4)$$

Customer demand is then sampled on each retail-demand link. If backlog mode is enabled, the effective demand $\tilde{D}_t^{(j,k)}$ includes the previous period's unmet demand; otherwise, unmet demand is treated as lost sales and is not carried forward. Retail shipments satisfy $S_t^{(j,k)} = \min\{\tilde{D}_t^{(j,k)}, X_{t+1}^{(j)}\}$, and the unfulfilled gap is recorded as $U_t^{(j,k)} = \tilde{D}_t^{(j,k)} - S_t^{(j,k)}$. Thus U_t is always tracked for penalty, service, and goodwill diagnostics, but it only becomes part of \tilde{D}_{t+1} in backlog configurations. These transition constraints ensure that neural policies, heuristics, and mathematical programming solvers are all evaluated under the same physical delays, inventory conservation, and capacity limits.

3.4 Reward and KPI Accounting

The objective of the agent is to maximize network-wide profitability. At time step t , the reward r_t is the sum of realized period profits over managed nodes. Let $M \subseteq V$ denote the set of managed nodes (retailers, distributors, and factories, excluding raw-material sources and end markets). Conditional on the realized demand and feasible filled orders in period t , the reward follows a standard additive inventory cost decomposition (Porteus, 2002):

$$\begin{aligned} r_t = \sum_{j \in M} P_t^{(j)} = \alpha^t \sum_{j \in M} \left[\underbrace{\sum_{k \in \text{succ}(j)} p_{jk} S_t^{(j,k)}}_{\text{SR}} - \underbrace{\sum_{i:(i,j) \in E_r} p_{ij} R_t^{(i,j)} - h_j X_{t+1}^{(j)}}_{\text{PC}} \right. \\ \left. - \underbrace{\sum_{i:(i,j) \in E_r} g_{ij} Y_{t+1}^{(i,j)}}_{\text{PHC}} - \underbrace{\frac{o_j}{v_j} \sum_{k \in \text{succ}(j)} S_t^{(j,k)}}_{\text{OC}} - \underbrace{\sum_{k:(j,k) \in E_d} b_{jk} U_t^{(j,k)}}_{\text{SP}} - \underbrace{\sum_{i:(i,j) \in E_r} K_{ij} \mathbf{1}\{R_t^{(i,j)} > 0\}}_{\text{FK}} \right]. \end{aligned} \quad (5)$$

The bracket labels denote sales revenue (SR), procurement cost (PC), node holding cost (HC), pipeline holding cost (PHC), operating cost (OC), shortage penalty (SP), and fixed ordering cost (FK). Here p_{jk} is the unit transfer or retail price on edge (j, k) , h_j is the node holding cost, g_{ij} is the inbound pipeline holding cost, o_j is the operating-cost coefficient, v_j is the production yield, b_{jk} is the per-unit shortage penalty, and K_{ij} is an optional fixed fee for a physically filled order on edge (i, j) . The factor $\alpha \in (0, 1]$ is the environment's financial profit-discount factor, distinct from any algorithm-specific discount used internally during RL training. Fixed ordering costs default to zero unless specified by the topology.

Because the reward is computed after demand realization and retail fulfillment, holding and pipeline costs accrue on post-step stocks X_{t+1} and Y_{t+1} , while shortage penalties accrue on end-of-period unfulfilled demand U_t . The fixed ordering

cost is triggered by $\mathbf{1}\{R_t^{(i,j)} > 0\}$, not by the raw request $a_t^{(i,j)}$; therefore a controller is not charged a setup fee for a request that cannot be physically filled because of upstream inventory, yield, or capacity constraints. The same decomposed terms are exported as benchmark KPIs, together with service level, fill rate, unfulfilled demand, average inventory, and bullwhip diagnostics.

3.5 Demand Processes and Goodwill Feedback

The environment extends classical stationary Poisson demand by supporting composable non-stationary perturbations: external empirical demand traces, linear trends, sinusoidal seasonality, step-function shocks, and noise scaling around the current mean. The demand engine can also accept raw time-series vectors, such as historical retail demand profiles, as the base realization path. Benchmark scenarios can therefore stress both predictable parametric non-stationarity (trend and seasonality) and highly irregular empirical regime shifts.

Additionally, we introduce an endogenous customer goodwill dynamic, motivated by service-dependent demand and goodwill-loss models in inventory theory (Schwartz, 1966; Olsen and Parker, 2008). When activated, the service level establishes an asymmetric feedback loop: end-of-period unfulfilled demand U_t degrades customer sentiment s_t , thereby scaling the mean of the next demand draw. The sentiment state evolves as:

$$s_{t+1} = \begin{cases} \max(s_{\min}, \gamma_{\text{drop}} \cdot s_t) & \text{if stockout at } t, \\ \min(s_{\max}, \gamma_{\text{rec}} \cdot s_t) & \text{otherwise,} \end{cases} \quad (6)$$

where $\gamma_{\text{drop}} = 0.90$, $\gamma_{\text{rec}} = 1.01$, $s_{\min} = 0.2$, and $s_{\max} = 2.0$. Here, a stockout event is triggered when aggregate unfulfilled demand across retail-demand links is strictly positive, $\sum_{(j,k) \in E_d} U_t^{(j,k)} > 0$. The effective demand mean for the next draw is $\lambda_{t+1} = s_{t+1} \bar{\lambda}_{t+1}$, where $\bar{\lambda}_{t+1}$ is the exogenous mean after any trend, seasonal, shock, or external-series effects. Because sentiment decays abruptly but recovers slowly (Fig. 3b), goodwill creates path-dependent non-stationarity: the same exogenous demand profile can generate different future demand trajectories depending on the policy’s past service failures. This provides a stress test for both learned policies and rolling-horizon OR baselines, because endogenous demand feedback couples present fulfillment decisions to future market size.

Proposition 1 (Goodwill Drift Threshold). *Consider a stationary service process with long-run no-stockout probability $\rho = \Pr(\text{no stockout at } t)$. Ignoring the reflecting floor and cap, the expected log-drift of goodwill is non-negative when*

$$\rho \geq \rho_{\min} = \frac{\ln(1/\gamma_{\text{drop}})}{\ln(1/\gamma_{\text{drop}}) + \ln(\gamma_{\text{rec}})} \approx 91.37\%.$$

Below this threshold, goodwill has negative multiplicative drift and is pushed toward the floor s_{\min} ; above it, goodwill tends to recover toward the cap s_{\max} .

This threshold is not an additional assumption in the simulator; it is a diagnostic interpretation of the asymmetric update rule under a stationary service process. It formalizes why goodwill scenarios sharply punish repeated service failures: repeated short-run stockouts can create persistent demand erosion unless future service reliability is high enough to offset the decay.

4 Experimental Setup and Baseline Analysis

This section instantiates the benchmark contract defined in Section 3. We evaluate the released scenario matrix across topology, demand regime, shortage treatment, goodwill feedback, information access, and controller family. The evaluation is organized around a canonical 22-scenario core grid, with four supplemental MARL-mode scenarios reported separately in the same merged artifact, yielding a 26-scenario audit matrix over 10 canonical seeds. The benchmark includes 29 registered non-LLM agent configurations (Oracle, rolling-horizon OR, heuristics, RL, hybrid, and imitation-learning variants) plus the full-matrix LLM-Policy-C baseline. Neural policies are implemented in PyTorch (Paszke et al., 2019) and trained using Stable-Baselines3 (Raffin et al., 2021); all methods are evaluated through the same CoreEnv transition, reward, action-bound, and KPI contract.

4.1 Evaluated Solution Families

Table 2 maps the evaluated roster into solution families and demand-visibility tiers. Following the information protocol defined in Section 3.1, architectural inductive bias is reported separately from access to demand-context information. This distinction is important because demand visibility can change both the available decision information and the optimization landscape faced during training; separating it from architecture prevents an informed model from being mistaken for an intrinsically better architecture. For learned policies, informed and blind variants are trained as separate checkpoints; information access is therefore treated as an experimental factor rather than assumed to provide monotonic improvement.

The roster consists of 29 registered non-LLM agent IDs plus the full-matrix LLM-Policy-C baseline. The Oracle is reported as a non-causal reference: a perfect-information LP in exogenous-demand settings and a clairvoyant simulation-optimization benchmark under endogenous goodwill. Rolling-horizon OR baselines are represented by MSSP and DLP;

classical heuristics provide interpretable industrial references; learned families cover flat-vector PPO/SAC, graph-message-passing PPO, Transformer PPO, residual RL, and imitation-learning variants. The LLM-Policy-C baseline is included as a bounded policy-parameter diagnostic for foundation-model reasoning, not as a replacement for specialized inventory controllers. Diagnostic PPO-MLP-v1 and PPO-MLP-raw ablations are retained in the released CSV but omitted from the condensed main tables. For reproducibility, the released CSV also preserves a few legacy implementation prefixes: GNN_V3 and GNN_V3_B correspond to PPO-GNN and PPO-GNN-B, respectively.

Table 2. Paradigm comparison of evaluated solution families. The canonical benchmark registers 29 non-LLM agent IDs (including Oracle and ablations) plus the full-matrix LLM-Policy-C baseline. Direct per-period LLM prompting variants are retained as diagnostics in the appendix.

Agent	Paradigm	Information Access	Solution Protocol
Oracle	Bound	Non-causal	Clairvoyant LP / fixed-point benchmark
MSSP / MSSP-I	SAA-RH OR	Blind / Informed	Multi-stage stochastic program
DLP / DLP-I	RH OR	Blind / Informed	Deterministic expected-value LP
Newsvendor / NV-I	Heuristics	Blind / Informed	Critical-Ratio (Arrow et al., 1951)
(s, S) / (s, S) -I	Heuristics	Blind / Informed	Reorder-point/order-up-to (Scarf, 1960)
ExpSmooth / ExpSmooth-I	Adapt. Heur.	Blind / Informed	Holt linear smoothing
Echelon / Echelon-I	Heuristics	Blind / Informed	Echelon-inspired base-stock (Clark and Scarf, 1960)
DAGger-B / DAGger-G	Imitation L.	Blind / Informed	Dataset Aggregation (Ross et al., 2011)
GNN-IL	Imitation L.	Graph states	Behavioral cloning + PPO fine-tuning
PPO-GNN / PPO-GNN-B	Advanced RL	Informed / Blind	Directed MPNN + PPO (Schulman et al., 2017; Gilmer et al., 2017; Veličković et al., 2018)
PPO-Transformer	Advanced RL	Informed	Node-Token Transformer + PPO (Vaswani et al., 2017; Schulman et al., 2017)
ST-PPO / ST-PPO-B	Advanced RL	Informed / Blind	Spatio-Temporal Transformer + PPO (Vaswani et al., 2017; Schulman et al., 2017; Zambaldi et al., 2019; Parisotto et al., 2020)
SAC / SAC-B	Deep RL	Informed / Blind	Soft Actor-Critic (Haarnoja et al., 2018)
Residual / Res.-B	Hybrid	Informed / Blind	PPO + Heuristic (Silver et al., 2018)
PPO-MLP / PPO-MLP-B	Standard RL	Informed / Blind	PPO (Schulman et al., 2017)
LLM-Policy-C	Foundation	Episode-level prompt	LLM strategy + deterministic controller (Quan and Liu, 2024)

Oracle (upper bound / clairvoyant heuristic). For exogenous demand, the Oracle is a perfect-information linear/mixed-integer program that observes the realized demand sequence before selecting a plan. The model is written in PuLP, a Python linear-programming modeling package, and solved with COIN-OR Branch-and-Cut (CBC) (Mitchell et al., 2011; Forrest and Lougee-Heimer, 2005) against the same inventory, pipeline, backlog, lead-time, capacity, and reward contract as the online agents. For endogenous goodwill, future demand is policy-dependent, so the Oracle is not a certified dynamic-programming optimum. We instead report it as a clairvoyant simulation-optimization benchmark using a bidirectional fixed-point procedure over pessimistic and optimistic demand traces.

Rolling-horizon LP baselines (MSSP, DLP). The Multi-Stage Stochastic Program (MSSP) (Birge and Louveaux, 2011) is implemented as a rolling-horizon sample-average approximation with non-anticipativity constraints. MSSP-I uses the informed future demand mean path, while MSSP estimates future demand from the causal history. The Deterministic LP (DLP) replaces the scenario tree with an expected-value trajectory, producing a cheaper but risk-neutral rolling baseline. Both solvers cap their horizon at the remaining episode length and re-solve online from the current simulator state.

Heuristics. The classical baselines are centralized, graph-aware adaptations rather than exact implementations of single-item textbook policies. Newsvendor uses a critical-ratio base-stock target (Arrow et al., 1951; Porteus, 2002); (s, S) uses a reorder-point/order-up-to batching rule (Scarf, 1960; Porteus, 2002); ExpSmooth uses Holt linear smoothing (Hyndman and Athanasopoulos, 2021); and EchelonApprox is a Clark–Scarf-inspired echelon base-stock approximation (Clark and Scarf, 1960), not an exact dynamic program. Informed variants use current demand parameters or variance information where available; blind variants estimate from realized history.

Imitation learning. DAGger-B and DAGger-G (Ross et al., 2011) evaluate GNN-based policies trained from expert demonstrations under blind and informed observation contracts, respectively. GNN-IL provides a separate behavioral-cloning-plus-PPO-finetuning diagnostic using the same directed graph feature extractor as PPO-GNN. We treat these as imitation-learning baselines and diagnostics for distribution shift, not as direct claims that imitation dominates the RL or OR families.

Deep RL and hybrid agents. All RL agents are trained using Stable-Baselines3 (Raffin et al., 2021). PPO-MLP uses standard Proximal Policy Optimization (Schulman et al., 2017) with a flat MLP policy. PPO-GNN replaces the MLP feature extractor with a directed edge-conditioned Message Passing Neural Network (MPNN) (Gilmer et al., 2017; Veličković et al., 2018) that processes the supply chain graph via bidirectional (upstream/downstream) message passing with edge features, attention-weighted aggregation, residual connections, LayerNorm, and BatchNorm. We introduce

two Transformer-based PPO variants: (i) **PPO-Transformer**, which treats each supply-chain node as a token and applies spatial self-attention (Vaswani et al., 2017); and (ii) **ST-PPO**, which extends PPO-Transformer with temporal frame stacking ($n=4$), creating (node \times timestep) tokens for joint spatio-temporal attention (Parisotto et al., 2020). SAC uses Soft Actor-Critic (Haarnoja et al., 2018). Residual RL adds a learned correction to a base-stock heuristic (Silver et al., 2018). Architecture details and hyperparameters are reported in the full appendix version.

Foundation-model baseline. To test whether a local foundation model can contribute useful inventory decisions without being queried at every period, LLM-Policy-C uses a Qwen2.5-1.5B-Instruct model once per episode to select bounded policy parameters for a deterministic controller. This “LLM as strategist, code as controller” setup is the only LLM variant included in the full 26-scenario matrix. Direct raw-action prompting and InvAgent-inspired staged prompts are retained as diagnostics in the full appendix version because they suffer from high latency and action-format failures.

Generalist training protocol. For the main PPO, SAC, Transformer, GNN, and Residual RL controllers, each reported checkpoint is a *single generalist model per (architecture \times topology)*, not a per-scenario specialist. During RL training, the topology is fixed (base or serial), while demand profile, goodwill, fulfillment mode, and noise scale are randomized at every episode reset via domain randomization. This produces one checkpoint per topology (e.g., `ppo-transformer_base.zip`, `st-ppo_serial.zip`). The imitation-learning diagnostics are also evaluated from fixed topology-level checkpoints: DAGger-G/B use graph imitation policies, while GNN-IL uses Oracle behavioral cloning followed by PPO fine-tuning on the canonical stationary training environment. Thus, GNN-IL should be read as an imitation diagnostic rather than as part of the domain-randomized RL training pool.

At evaluation time, each learned checkpoint is tested on the full 22-scenario fixed grid across 10 canonical seeds (220 episodes per agent), using deterministic inference. Four additional MARL-mode scenarios are evaluated separately (documented in the full appendix version), bringing the total to 26 scenarios (260 episodes). This design explicitly imposes a *generalization tax*: learned policies must deploy across diverse regimes without scenario-specific retraining, while OR solvers and heuristics adapt online to the current state and, in informed variants, to current demand parameters. Reported neural performance therefore reflects cross-regime deployment robustness, not scenario-tuned optimality.

4.2 Scenario Matrix and Evaluation Protocol

The main benchmark uses a curated 22-scenario core matrix (Table 3). The design is intentionally representative rather than exhaustive: it combines topology, demand regime, endogenous feedback, and fulfillment mode to cover stress patterns common in the inventory-control literature while remaining small enough for cross-paradigm evaluation over many agents and seeds. Starting from the conceptual factorial design (2 topologies \times 4 demand regimes \times 2 goodwill modes \times 2 fulfillment modes = 32), we apply two exclusions. First, stationary and M5 external-trace profiles are not paired with endogenous goodwill, because goodwill is designed to stress service-dependent non-stationarity (-8). Second, the M5 trace is evaluated only under backlog fulfillment, avoiding an interpretation of observed retail sales as an uncensored lost-sales demand process (-2). The M5 scenario is derived from the real `sales_train_evaluation` item-store panel: we select a 30-day item-store window with high rolling coefficient of variation subject to minimum activity filters, scale the observed unit-sales path to the benchmark mean demand level ($\bar{d} = 20$), and replay it deterministically as an external demand trace. This makes the scenario a real-data stress test rather than a claim that one M5 item is representative of all Walmart demand. The canonical M5 rows use the M5 panel for terminal demand only: calendar features, SNAP/event indicators, sell-price histories, and Walmart’s unobserved replenishment network are not treated as observed supply-chain physics. Lead times, capacities, inventory costs, and shortage penalties remain controlled benchmark parameters. A separate adapter can infer a hierarchy-based planning DAG from M5 metadata, but such hierarchy-inferred topologies change the action space and are reported as custom topology experiments rather than replacements for the canonical base/serial M5 rows.

The resulting 22 core scenarios consist of 16 synthetic non-stationary stress tests, four stationary paper-replication scenarios, and two M5-derived external-trace scenarios. Four additional MARL-mode rows reuse non-goodwill backlog synthetic scenarios with the MARL evaluation flag enabled; these supplemental rows bring the merged artifact to 26 scenarios and are reported separately where relevant. The core and supplemental rows are enumerated in the full appendix version.

Table 3. Core scenario axes for the 22-scenario evaluation matrix. The four supplemental MARL-mode rows use the same topology and demand axes but are not part of the core 22-scenario aggregate unless explicitly stated.

Axis	Configurations	Benchmarking Purpose
Topology (2)	Default network (9-node), Serial (5-node)	Contrasts branching/merging allocation and capacity interactions with linear pipeline delays.
Demand (4)	Stationary, M5-derived volatile, Trend+Seasonal, Trend+Seas.+Shock	Tests stationary control, external-trace robustness, and composable non-stationary distribution shifts.
Dynamics (2)	Exogenous, Endogenous Goodwill	Evaluates resilience against service-level feedback loops in synthetic non-stationary settings.
Fulfillment (2)	Backlog, Lost Sales	Shifts the penalty landscape from accumulated debt to immediate loss.

4.3 Main Benchmark Results and Compute Trade-off

Table 4 consolidates the 22-scenario core benchmark into three interpretable regimes: stationary demand, non-stationary exogenous demand, and endogenous-goodwill demand. The dominant quality result is that informed stochastic programming (MSSP-I) is the strongest causal non-Oracle baseline, reaching approximately **95%** of Oracle profit on the core grid. This is not a claim that stochastic programming is universally deployment-friendly: MSSP-I requires repeated rolling-horizon solves and informed forecast access. Rather, it provides the empirical quality ceiling among causal methods in this benchmark.

The learned-policy frontier is different. PPO-Transformer is the strongest fast learned policy in aggregate, reaching approximately **75%** of Oracle across the core grid, while Residual RL remains close at approximately **73%**. DAgger-B is highly effective in-distribution, capturing approximately **95%** of Oracle under stationary demand, but its non-stationary performance falls to 33%, illustrating imitation learning’s sensitivity to distribution shift. SAC is a cautionary counterexample: the informed checkpoint has negative stationary performance on average and is dominated by its blind counterpart, indicating checkpoint instability rather than a monotone benefit from richer observations. GNN-IL is therefore retained as a diagnostic imitation baseline rather than a headline method. Finally, the full-matrix LLM-Policy-C baseline reaches approximately **60%** of Oracle on the core grid: competitive with several classical and neural baselines, but with much higher latency than specialized learned policies.

Table 4 reports the corresponding computational costs. These timings should be interpreted as evaluation latency on the reported hardware, not universal wall-clock constants; they mainly show the amortization pattern whereby trained policies replace repeated optimization with a forward pass or a lightweight heuristic correction.

Table 4. Core performance and computational cost by paradigm. Performance columns report scenario-wise % of Oracle profit, averaged over the 22-scenario core grid (mean \pm sample cross-scenario SD; these are heterogeneity summaries, not seed-level confidence intervals). Inference time is mean seconds per episode on the same hardware; speed-up is relative to blind MSSP.

Category	Agent	Stat. (4)	Non-S. (10)	End. (8)	All	s/ ep	Speed
<i>Bound</i>	Oracle	100	100	100	100	0.84	—
<i>Rolling-Horizon OR</i>	MSSP	92 \pm 5	61 \pm 26	58 \pm 7	66 \pm 22	10.28	1 \times
	MSSP-I	97 \pm 1	99 \pm 1	89 \pm 3	95\pm5	7.68	1.3 \times
	DLP	78 \pm 15	36 \pm 29	52 \pm 11	49 \pm 26	1.06	9.7 \times
	DLP-I	80 \pm 15	50 \pm 32	58 \pm 18	58 \pm 27	1.00	10.2 \times
<i>Heuristics</i>	News vendor	83 \pm 7	46 \pm 32	56 \pm 7	56 \pm 25	0.049	210 \times
	(s, S)	86 \pm 2	51 \pm 32	61 \pm 7	61 \pm 25	0.032	317 \times
	ExpSmooth	84 \pm 5	45 \pm 32	55 \pm 7	56 \pm 26	0.037	281 \times
	Echelon	84 \pm 5	50 \pm 43	55 \pm 6	58 \pm 31	0.058	176 \times
	Echelon-I	88 \pm 3	67 \pm 17	71 \pm 6	72 \pm 14	0.054	192 \times
<i>Imit. L.</i>	DAgger-B	95 \pm 2	33 \pm 25	59 \pm 12	53 \pm 29	0.273	38 \times
	GNN-IL	84 \pm 7	3 \pm 54	25 \pm 26	26 \pm 48	0.275	37 \times
<i>Deep RL</i>	PPO-MLP	77 \pm 9	56 \pm 35	62 \pm 23	62 \pm 28	0.132	78 \times
	PPO-GNN	73 \pm 3	57 \pm 35	62 \pm 23	61 \pm 27	0.305	34 \times
	PPO-Transformer	74 \pm 6	77 \pm 13	71 \pm 12	75 \pm 12	0.229	45 \times
	ST-PPO	69 \pm 2	59 \pm 32	64 \pm 20	63 \pm 24	0.269	38 \times
	SAC	-13 \pm 53	35 \pm 47	73 \pm 13	40 \pm 49	0.135	76 \times
<i>Hybrid</i>	Residual	87 \pm 4	68 \pm 17	73 \pm 6	73 \pm 14	0.223	46 \times
<i>Foundation</i>	LLM-Policy-C	77 \pm 2	54 \pm 22	58 \pm 17	60 \pm 20	8.150	1.3 \times

Compute-quality interpretation. Table 4 shows that solution quality and latency do not move together monotonically. MSSP-I provides the strongest causal quality benchmark, but blind MSSP still requires roughly 10.3 seconds per 30-period episode on the reported hardware because it re-solves a sampled scenario tree online. DLP is faster (~ 1.1 s/episode) but sacrifices scenario hedging and performs substantially worse under stochastic non-stationarity.

Trained neural policies amortize this repeated optimization into offline training plus fast evaluation. PPO-Transformer reaches approximately 75% of Oracle profit while running in ~ 0.229 s/episode, about 45 \times faster than blind MSSP. PPO-MLP is also lightweight (~ 0.132 s/episode) but gives up some quality, while graph and residual policies incur additional feature extraction or heuristic-evaluation overhead. Residual RL is the strongest hybrid policy in the table by scenario-wise percentage (73% of Oracle), while its inference latency (~ 0.223 s/episode) is comparable to the Transformer policies and well below DLP.

Training time should therefore be interpreted as an offline amortized cost, not as part of every episode’s latency. For a learned policy used over N future episodes, the effective computational cost is $C_{\text{train}}/N + C_{\text{infer}}$. Training costs are not included in the compact table because several legacy pretrained artifacts lack retained training logs; those artifacts are evaluated from shipped weights but are not used for exact training-time claims. This favors OR solvers and heuristics for one-off planning, but favors reusable generalist policies when the same trained controller is deployed repeatedly across stores, SKUs, seeds, or rolling operational cycles. Specialist policies face a higher effective cost whenever a separate checkpoint must be trained for each scenario.

The LLM-Policy-C baseline occupies a different point on this frontier: it avoids per-period language-model calls by querying once per episode, but still averages roughly 8.2 s/episode. This is slightly faster than blind MSSP in the final artifact but far slower than DLP, heuristics, and specialized learned policies. Its role is therefore diagnostic and strategic rather than latency-competitive. Overall, the compute results support an amortization narrative, not a universal neural dominance claim: specialized learned policies can be much faster than rolling-horizon stochastic programming, but the magnitude depends strongly on architecture and whether the controller invokes graph, heuristic, or language-model components.

4.4 Information Access and Architecture Effects

Where paired variants are available, we evaluate agents under a common **information parity protocol**. Blind variants estimate demand from observation history, while informed variants receive the current scenario’s demand parameters through the same environment-native feature contract. For learned policies, blind and informed results should be read as separate trained checkpoints rather than as a guaranteed monotone improvement from adding features: the additional information can also change optimization dynamics and generalization.

Table 5 shows that the value of information is largest when the downstream algorithm can use it structurally. MSSP gains 29.2 percentage points because its scenario tree is centered on the correct demand process; DLP gains only 9.2 points because its expected-value LP still ignores variance. Classical heuristics benefit when their target calculations can use demand-parameter information directly, with double-digit gains of 14.1 points for Newsvendor, 14.0 points for EchelonApprox, and 10.0 points for (s, S) . In contrast, the reactive exponential smoothing baseline gains only 0.7 points.

The learned-policy pairs are less monotonic. Residual RL improves by 15.2 points when informed features are available, while PPO-GNN and ST-PPO change by roughly one point on the core grid. SAC is the counterexample: its blind checkpoint exceeds the informed checkpoint by 19.9 points, driven by poor serial-topology training outcomes for the informed SAC model. Thus, information access is an essential control dimension, but the empirical ranking reflects an interaction among information, architecture, and training stability rather than information alone.

Table 5. Value of information for selected paired methods (scenario-wise % of Oracle profit, averaged over the 22 core scenarios).

Agent	Blind (%)	Informed (%)	Δ (pp)
MSSP	65.7	94.9	+29.2
DLP	49.2	58.4	+9.2
Newsvendor	56.2	70.3	+14.1
(s, S)	61.1	71.1	+10.0
ExpSmooth	55.8	56.5	+0.7
Echelon	58.4	72.4	+14.0
Residual	58.0	73.2	+15.2
SAC	59.7	39.9	-19.9

Topology-transfer summary. We treat topology transfer as an architectural stress test rather than part of the main 22-scenario ranking. A Residual GCN-Pool policy trained on the default 9-node topology retains positive profit when deployed zero-shot on four unseen graphs, preserving 41–84% of the Newsvendor heuristic’s profit depending on structural similarity. However, the transfer experiments also expose a service-level failure: the fixed-size action head can generate profitable inventory behavior while failing to route material reliably to new retail edges. For this reason, the full transfer ladder, statistical tests, and operational KPI decomposition are reported in the full appendix version; the main text uses the result primarily to motivate topology-aware action decoding.

4.5 Stress Tests and Foundation-Model Policy Baseline

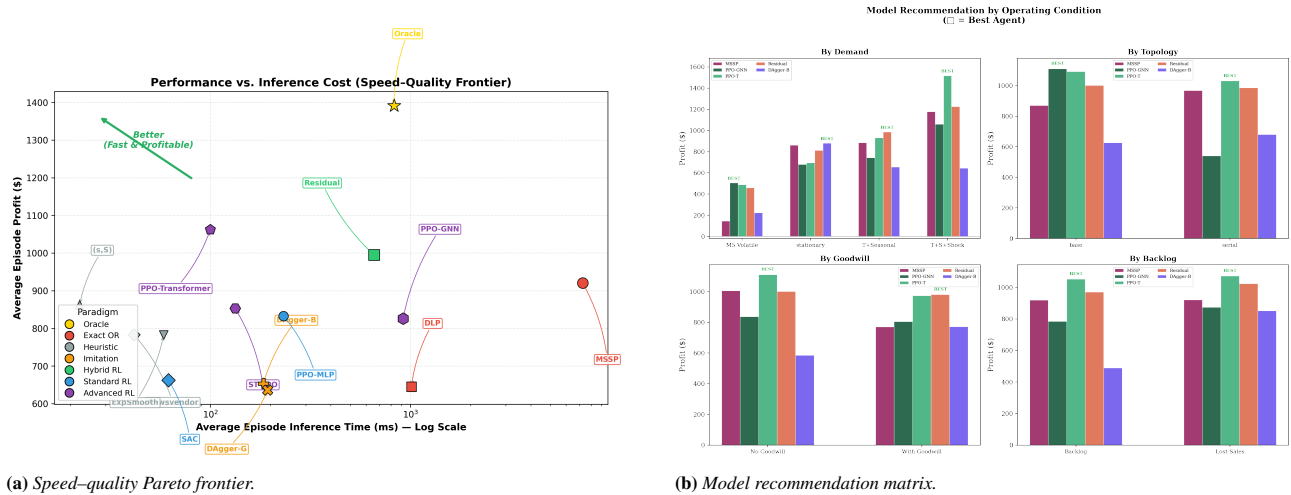
The stress-test regimes explain why the aggregate ranking should not be read as a single universal ordering. Under non-stationary exogenous demand, MSSP-I remains near the Oracle because its scenario tree hedges against future demand paths, while DLP-I can under-stock sharply on serial topologies because it optimizes only an expected-value path. DAgger-B provides the opposite lesson: it reaches 94.6% of Oracle in stationary regimes but drops under trend, seasonality, and shocks, consistent with imitation learning’s sensitivity to covariate shift.

Endogenous goodwill creates a different stressor because future demand depends on the service path induced by the policy. In the eight goodwill core scenarios, blind MSSP averages 57.9% of Oracle, while MSSP-I recovers to 89.1% by centering its scenario tree on the informed demand path. The strongest learned and hybrid policies remain meaningful but below MSSP-I: Residual RL reaches 73.0%, SAC 72.8%, and PPO-Transformer 71.4% of Oracle. These results indicate that learned policies can buffer against service-feedback dynamics, but they do not replace informed stochastic programming in this benchmark. They are also consistent with the drift interpretation in Proposition 1: goodwill rows remain severe because even policies with high fill rates can experience no-stockout probabilities below the 91.37% recovery threshold, so occasional service failures continue to exert downward pressure on sentiment.

The foundation-model experiments add a final stress test around action formatting and latency. Direct raw-action prompting with the local Qwen2.5-1.5B-Instruct model (Qwen Team, 2024) produced over-ordering, parse/shape

failures, and multi-minute episodes. The full-matrix LLM-Policy-C variant instead queries the model once per episode for bounded base-stock multipliers and delegates execution to deterministic controllers. This stabilizes the action format and reaches about 60% of Oracle on the core grid. It averages roughly 8.2 seconds per episode on the core grid and about 9.0 seconds over all 26 rows, making it slightly faster than blind MSSP but far slower than DLP, heuristics, and specialized learned policies. LLMs are therefore best interpreted here as strategic policy-parameter generators rather than high-frequency inventory controllers.

Fig. 4a visualizes the speed–quality frontier, while Fig. 4b supports method selection by decomposing performance along each scenario axis. The full appendix version provides scenario-level heatmaps, training curves, transfer diagnostics, and detailed LLM diagnostics.



(a) Speed–quality Pareto frontier.

(b) Model recommendation matrix.

Figure 4. (a) Average episode profit vs. inference time (log scale), illustrating the separation between rolling-horizon OR quality, fast learned-policy inference, and the slower LLM-policy baseline. (b) Model recommendation by operating condition. Four panels decompose mean profit by demand regime, topology, goodwill mode, and fulfillment policy. “BEST” labels mark the top non-Oracle agent.

5 Discussion, Limitations, and Future Directions

5.1 Discussion

The central lesson from `gym-invmgmt` is not that one paradigm dominates inventory control. Instead, the benchmark exposes a deployment trade-off among information access, uncertainty modeling, architectural bias, and computational amortization. Informed stochastic programming provides the strongest causal non-Oracle quality benchmark: MSSP-I achieves 94.9% of Oracle on the 22-scenario core grid. Its advantage over DLP-I shows that the value of OR in this setting is not merely optimization over a network flow model, but explicit scenario hedging under stochastic non-stationarity.

Learned policies occupy a different part of the frontier. PPO-Transformer and Residual RL reach 73–75% of Oracle on the core grid, below MSSP-I but with substantially lower online latency. This does not support a blanket claim that neural policies replace rolling-horizon solvers. It supports a more specific claim: once trained, generalist neural controllers can amortize decision making across many episodes, stores, seeds, or rolling deployments, making them attractive when repeated online optimization is too slow or operationally cumbersome. The strongest learned methods are therefore best viewed as fast reusable approximations, not as universal substitutes for informed stochastic programming.

The benchmark also shows why information access must be treated as an experimental factor rather than a slogan. Informed demand parameters help MSSP substantially and provide double-digit gains for variance-sensitive heuristics such as NewsVendor, EchelonApprox, and (s, S) , but they do not guarantee monotonic gains for learned agents. SAC, for example, is worse in its informed variant because checkpoint quality and optimization stability interact with the feature contract. This is a useful negative result: inventory benchmarks should report blind and informed variants explicitly, because additional information can change both what the policy knows and how difficult the policy is to train.

Finally, the diagnostic baselines clarify failure modes that aggregate profit alone would hide. DAgger-B imitates Oracle-like behavior under stationary and M5 external-trace demand, but degrades under trend/seasonal shock regimes, illustrating covariate shift. GNN-IL is therefore retained as a diagnostic BC-to-PPO pipeline rather than a headline method. LLM-Policy-C is stable enough for the full scenario matrix when used as a low-frequency policy-parameter generator, but it remains slower and weaker than the best OR, heuristic, and learned controllers; direct per-period LLM action generation is still brittle. The topology-transfer experiments similarly show partial profit transfer but service-level collapse, suggesting that graph encoders alone are insufficient without topology-native action decoders.

5.2 Methodological Limitations

The results should be read as controlled benchmark evidence rather than as universal rankings. The first limitation is **scenario and topology scope**: the 22-scenario core grid covers patterns that are common in the literature—serial and default multi-echelon topologies, stationary and non-stationary demand, backlog and lost-sales fulfillment, and endogenous

goodwill feedback—but it is not a statistically representative sample of all supply chains. The value of the grid is therefore comparative control: it shows how method rankings change when specific assumptions are varied under identical simulator mechanics.

A second limitation concerns **external data mapping**. The M5 rows inject a real item-store sales trace as terminal demand, but they do not reconstruct Walmart’s physical replenishment network. Calendar features, SNAP/event indicators, sell-price histories, upstream lead times, capacities, and costs are not treated as observed logistics variables in the canonical M5 rows. The released adapters can infer planning DAGs from public retail hierarchies, but those graphs should be interpreted as dataset-derived stress tests unless external logistics data are added.

The evaluation also separates **seed-level evaluation uncertainty** from full training-run uncertainty. Each scenario is evaluated over 10 canonical seeds, while many learned checkpoints are trained once per topology and architecture. This design makes the released comparison auditable, but it does not replace multi-seed training, confidence intervals over checkpoint selection, or architecture-specific hyperparameter sweeps. Those additions would be necessary to make claims about training stability rather than about the deployed checkpoints in the benchmark artifact.

Finally, the benchmark deliberately compares **deployment roles** that are not mathematically identical. Oracle is non-causal; MSSP-I uses informed demand parameters; learned policies act through featurized observations; heuristics encode structural assumptions; and LLM-Policy-C uses low-frequency policy-parameter generation. This role asymmetry is explicit rather than accidental, but it means the results should not be read as if every controller solved the same information-relaxed problem. The same caution applies to endogenous goodwill: for exogenous demand, the Oracle is a perfect-foresight LP benchmark, whereas under goodwill future demand depends on the policy-induced service path. In those rows, the Oracle is a clairvoyant simulation-optimization benchmark rather than a certified global upper bound.

5.3 Open Challenges and Future Work

These limitations point to extensions that build directly on the released benchmark. At the evaluation layer, future releases should add multi-seed training, bootstrap confidence intervals, paired non-parametric tests, vector-valued rewards for multi-objective trade-offs (Felten et al., 2023), and a JAX-native backend for scalable rollouts (Bonnet et al., 2024); this release prioritizes checkpoint-level auditability. The most immediate technical challenge is **topology-aware action decoding**. The transfer experiments show that graph encoders can preserve positive profit across unseen graphs, but fixed-size action heads do not reliably route material to new retail edges. Future graph policies should make action generation topology native through per-edge decoders, pointer mechanisms (Vinyals et al., 2015), or edge-conditioned action heads.

A second direction is **hybrid OR-learning control**. This study compares MSSP-I, DLP, heuristics, RL, residual RL, imitation, and LLM policies as distinct paradigms; Residual RL is already a first integration step because it learns a correction on top of a heuristic controller. Future work can deepen the coupling by using stochastic programs to produce scenario-aware base-stock or flow targets and by using learned policies to warm-start or approximate rolling-horizon DLP/MSSP. Such hybrids would combine OR quality references with amortized neural speed.

The benchmark also leaves room for **richer supply-chain physics and data adapters**. Beyond the current DAGs, backlog/lost-sales regimes, goodwill, fixed costs, and empirical traces, extensions should stress heavy-tailed or mixture demand, longer 100–365 period horizons, stochastic lead times, random yields, disruptions, shared resources, liquidity limits, multi-product substitution, and price/calendar covariates.

Finally, **foundation-model controllers** remain an open research frontier rather than a solved benchmark component. The LLM experiments suggest that raw per-period action generation is too slow and brittle, whereas episode-level strategy extraction is more viable. Future work should test constrained decoding, tool-verified JSON schemas, retrieval over inventory histories, and hybrid LLM–OR policies where deterministic controllers enforce feasibility and action bounds.

5.4 Conclusion

Taken together, the results argue for benchmark-driven method selection. Informed stochastic programming is the strongest quality reference when its information and compute requirements are acceptable; heuristics remain highly competitive and transparent; learned policies offer fast amortized decision making; residual and imitation methods expose useful hybridization paths; and foundation models are currently better suited to bounded strategy generation than direct control. `gym-invmgmt` provides a common graph-based environment contract for comparing these choices under identical simulator mechanics, making the trade-offs visible rather than implicit.

CRedit Authorship Contribution Statement

Reza Barati: Conceptualization, Methodology, Software, Validation, Formal Analysis, Investigation, Data Curation, Writing – Original Draft, Visualization. **Qinmin Vivian Hu:** Supervision, Writing – Review & Editing, Resources, Project Administration.

Funding

This research did not receive any specific grant from funding agencies in the public, commercial, or not-for-profit sectors.

Declaration of Competing Interests

The authors declare that they have no known competing financial interests or personal relationships that could have appeared to influence the work reported in this paper.

Code and Data Availability

The benchmark source code, scenario definitions, evaluation scripts, figure-generation utilities, and canonical merged result artifacts are available at <https://github.com/r2barati/gym-invmgmt-paper>. A standalone Gymnasium environment package is maintained at <https://github.com/r2barati/gym-invmgmt>. Trained policy checkpoints and matching normalization statistics are archived separately on Hugging Face at <https://huggingface.co/datasets/rezabarati/gym-invmgmt-weights>. The external retail datasets used for adapter validation are not redistributed; scripts are provided to download them from their original public sources.

References

- Kenneth J. Arrow, Theodore Harris, and Jacob Marschak. Optimal inventory policy. *Econometrica*, 19(3):250–272, 1951.
- Bharathan Balaji, Jordan Bell-Masterson, Enes Bilgin, Andreas Damianou, Pablo Moreno Garcia, Arpit Jain, et al. ORL: Reinforcement learning benchmarks for online stochastic optimization problems. *arXiv preprint arXiv:1911.10641*, 2020.
- Gah-Yi Ban and Cynthia Rudin. The big data newsvendor: Practical insights from machine learning. *Operations Research*, 67(1):90–108, 2019.
- Richard Bellman. *Dynamic Programming*. Princeton University Press, Princeton, NJ, 1957.
- John R. Birge and François Louveaux. *Introduction to Stochastic Programming*. Springer, New York, 2nd edition, 2011.
- Clément Bonnet, Daniel Luo, Donal Byrne, Shikha Surana, Sasha Abramowitz, Paul Duckworth, Vincent Coyette, Laurence I. Midgley, Elshadai Tegegn, Tristan Kalloniatis, Omayma Mahjoub, Matthew Macfarlane, Andries P. Smit, Nathan Grinsztajn, Raphael Boige, Cemlyn N. Waters, Mohamed A. Mimouni, Ulrich A. Mbou Sob, Ruan de Kock, Siddarth Singh, Daniel Furelos-Blanco, Victor Le, Arnu Pretorius, and Alexandre Laterre. Jumanji: A diverse suite of scalable reinforcement learning environments in JAX. In *International Conference on Learning Representations*, 2024. URL <https://openreview.net/forum?id=C4CxQmp9wc>.
- Robert N. Boute, Joren Gijsbrechts, Willem van Jaarsveld, and Niel Vanvuchelen. Deep reinforcement learning for inventory control: A roadmap. *European Journal of Operational Research*, 298(2):401–412, 2022.
- Greg Brockman, Vicki Cheung, Ludwig Pettersson, Jonas Schneider, John Schulman, Jie Tang, and Wojciech Zaremba. OpenAI Gym. *arXiv preprint arXiv:1606.01540*, 2016.
- Sara Charaf, Duygu Taş, Simme Douwe P. Flapper, and Tom Van Woensel. A matheuristic for the two-echelon inventory-routing problem. *Computers & Operations Research*, 171:106778, 2024. doi: 10.1016/j.cor.2024.106778.
- Jen-Ming Chen and Tsung-Hui Chen. The multi-item replenishment problem in a two-echelon supply chain: the effect of centralization versus decentralization. *Computers & Operations Research*, 32:3191–3207, 2005. doi: 10.1016/j.cor.2004.05.007.
- Andrew J. Clark and Herbert Scarf. Optimal policies for a multi-echelon inventory problem. *Management Science*, 6(4):475–490, 1960.
- Florian Felten, Lucas N. Alegre, Ann Nowé, Ana L. C. Bazzan, El Ghazali Talbi, Grégoire Danoy, and Bruno C. da Silva. A toolkit for reliable benchmarking and research in multi-objective reinforcement learning. In *Advances in Neural Information Processing Systems*, volume 36, 2023. URL https://proceedings.neurips.cc/paper_files/paper/2023/hash/4aa8891583f07ae200ba07843954caeb-Abstract-Datasets_and_Benchmarks.html.
- John Forrest and Robin Lougee-Heimer. CBC user guide. In *Emerging Theory, Methods, and Applications*, INFORMS Tutorials in Operations Research, pages 257–277. INFORMS, 2005. doi: 10.1287/educ.1053.0020.
- Yanran Gao and Shuning Chen. Deep reinforcement learning for multi-echelon supply chain management under demand uncertainty. *arXiv preprint arXiv:2003.11485*, 2020.
- Ilaria Giannoccaro and Pierpaolo Pontrandolfo. Inventory management in supply chains: a reinforcement learning approach. *International Journal of Production Economics*, 78(2):153–161, 2002.
- Joren Gijsbrechts, Robert N. Boute, Jan A. Van Mieghem, and Dennis J. Zhang. Can deep reinforcement learning improve inventory management? performance on lost sales, dual-sourcing, and multi-echelon problems. *Manufacturing & Service Operations Management*, 24(3):1349–1368, 2022.
- Justin Gilmer, Samuel S. Schoenholz, Patrick F. Riley, Oriol Vinyals, and George E. Dahl. Neural message passing for quantum chemistry. In *Proceedings of the 34th International Conference on Machine Learning (ICML)*, pages 1263–1272, 2017.

- Stephen C. Graves and Sean P. Willems. Optimizing strategic safety stock placement in supply chains. *Manufacturing & Service Operations Management*, 2(1):68–83, 2000.
- Tuomas Haarnoja, Aurick Zhou, Pieter Abbeel, and Sergey Levine. Soft actor-critic: Off-policy maximum entropy deep reinforcement learning with a stochastic actor. In *Proceedings of the 35th International Conference on Machine Learning (ICML)*, pages 1861–1870, 2018.
- Ford W. Harris. How many parts to make at once. *Factory, The Magazine of Management*, 10(2):135–136, 152, 1913.
- Christian D. Hubbs, Hector D. Perez, Owais Sarwar, Nikolaos V. Sahinidis, Ignacio E. Grossmann, and John M. Wassick. OR-Gym: A reinforcement learning library for operations research problems. *arXiv preprint arXiv:2008.06319*, 2020.
- Rob J. Hyndman and George Athanasopoulos. *Forecasting: Principles and Practice*. OTexts, Melbourne, Australia, 3rd edition, 2021. URL <https://otexts.com/fpp3/>.
- Lorenz Kemmer, Heinrich von Kleist, Frédéric de Rochebouët, Robert Birke, and Lydia Y. Chen. Reinforcement learning for supply chain optimization. In *European Workshop on Reinforcement Learning (EWRL)*, 2018.
- Nikhil Kotecha and Antonio del Rio Chanona. Leveraging graph neural networks and multi-agent reinforcement learning for inventory control in supply chains. *Computers and Chemical Engineering*, 199:109111, 2025.
- Rémi Leluc, Elie Kadoche, Antoine Bertonecello, and Sébastien Gourvéneec. MARLIM: Multi-agent reinforcement learning for inventory management. In *NeurIPS Workshop on Reinforcement Learning for Real Life (RLRealLife)*, 2022. arXiv:2308.01649.
- Dhruv Madeka, Kari Torkkola, Carson Eisenach, Anna Luo, Dean P. Foster, and Sham M. Kakade. Deep inventory management. *arXiv preprint arXiv:2210.03137v3*, 2022.
- Hardik Meisheri, Nasrin Nahida Sultana, Mayank Baranwal, Vinita Baniwal, Somjit Nath, Balaraman Ravindran, and Harshad Khadilkar. Scalable multi-product inventory control with lead time constraints using reinforcement learning. *Neural Computing and Applications*, 34(3):1735–1757, 2022. doi: 10.1007/s00521-021-06129-w.
- Stuart Mitchell, Michael O’Sullivan, and Iain Dunning. PuLP: A linear programming toolkit for Python, 2011. URL <https://github.com/coin-or/pulp>.
- Tava Lennon Olsen and Rodney P. Parker. Inventory management under market size dynamics. *Management Science*, 54(10):1805–1821, 2008. doi: 10.1287/mnsc.1080.0889.
- Afshin Oroojlooyjadid, MohammadReza Nazari, Lawrence V. Snyder, and Martin Takáč. A deep Q-network for the beer game: Deep reinforcement learning for inventory optimization. *Manufacturing & Service Operations Management*, 24(1):285–304, 2022.
- Emilio Parisotto, Francis Song, Jack Rae, Razvan Pascanu, Caglar Gulcehre, Siddhant Jayakumar, Max Jaderberg, Raphaël Lopez Kaufman, Aidan Clark, Seb Noury, Matthew Botvinick, Nicolas Heess, and Raia Hadsell. Stabilizing transformers for reinforcement learning. In *Proceedings of the 37th International Conference on Machine Learning*, volume 119 of *Proceedings of Machine Learning Research*, pages 7487–7498. PMLR, 2020. URL <https://proceedings.mlr.press/v119/parisotto20a.html>.
- Adam Paszke, Sam Gross, Francisco Massa, Adam Lerer, James Bradbury, Gregory Chanan, Trevor Killeen, Zeming Lin, Natalia Gimelshein, Luca Antiga, et al. PyTorch: An imperative style, high-performance deep learning library. In *Advances in Neural Information Processing Systems (NeurIPS)*, volume 32, pages 8024–8035, 2019.
- Hector D. Perez, Christian D. Hubbs, Can Li, and Ignacio E. Grossmann. Algorithmic approaches to inventory management optimization. *Processes*, 9(1):102, 2021.
- Evan L. Porteus. *Foundations of Stochastic Inventory Theory*. Stanford University Press, 2002.
- Martin L. Puterman. *Markov Decision Processes: Discrete Stochastic Dynamic Programming*. John Wiley & Sons, New York, 1994.
- Meng Qi, Yuanyuan Shi, Yongzhi Qi, Chenxin Ma, Rong Yuan, Di Wu, and Zuo-Jun Max Shen. A practical end-to-end inventory management model with deep learning. *Management Science*, 69(2):759–773, 2023.
- Yinzhu Quan and Zefang Liu. InvAgent: A large language model based multi-agent inventory management system. *arXiv preprint arXiv:2407.11384v1*, 2024.
- Qwen Team. Qwen2.5 technical report. *arXiv preprint arXiv:2412.15115*, 2024. doi: 10.48550/arXiv.2412.15115.

- Antonin Raffin, Ashley Hill, Adam Gleave, Anssi Kanervisto, Maximilian Ernestus, and Noah Dormann. Stable-Baselines3: Reliable reinforcement learning implementations. *Journal of Machine Learning Research*, 22(268):1–8, 2021.
- Benjamin Rolf, Ilya Jackson, Matthias Müller, Sebastian Lang, Tobias Reggelin, and Dmitry Ivanov. A review on reinforcement learning algorithms and applications in supply chain management. *International Journal of Production Research*, 61(20):7151–7179, 2023.
- Stéphane Ross, Geoffrey J. Gordon, and J. Andrew Bagnell. A reduction of imitation learning and structured prediction to no-regret online learning. In *Proceedings of the 14th International Conference on Artificial Intelligence and Statistics (AISTATS)*, pages 627–635, 2011.
- Herbert Scarf. A min-max solution of an inventory problem. In *Studies in the Mathematical Theory of Inventory and Production*, pages 201–209. Stanford University Press, Stanford, CA, 1958.
- Herbert Scarf. The optimality of (S,s) policies in the dynamic inventory problem. In Kenneth J. Arrow, Samuel Karlin, and Patrick Suppes, editors, *Mathematical Methods in the Social Sciences*, pages 196–202. Stanford University Press, Stanford, CA, 1960.
- John Schulman, Filip Wolski, Prafulla Dhariwal, Alec Radford, and Oleg Klimov. Proximal policy optimization algorithms. *arXiv preprint arXiv:1707.06347*, 2017.
- Benjamin L. Schwartz. A new approach to stockout penalties. *Management Science*, 12(12):B538–B544, 1966. doi: 10.1287/mnsc.12.12.B538.
- Tom Silver, Kelsey Allen, Josh Tenenbaum, and Leslie Kaelbling. Residual policy learning. In *Robotics: Science and Systems XIV*, 2018.
- C. R. Puppala Sridhar, C. R. Vishnu, and R. Sridharan. Simulation of inventory management systems in retail stores: A case study. *Materials Today: Proceedings*, 47:5130–5134, 2021. doi: 10.1016/j.matpr.2021.05.314.
- Mark Towers, Ariel Kwiatkowski, Jordan Terry, John U. Balis, Gianluca De Cola, Tristan Deleu, et al. Gymnasium: A standard interface for reinforcement learning environments. In *Thirty-seventh Conference on Neural Information Processing Systems Datasets and Benchmarks Track*, 2023.
- Ashish Vaswani, Noam Shazeer, Niki Parmar, Jakob Uszkoreit, Llion Jones, Aidan N. Gomez, Łukasz Kaiser, and Illia Polosukhin. Attention is all you need. In *Advances in Neural Information Processing Systems (NeurIPS)*, volume 30, pages 5998–6008, 2017.
- Petar Veličković, Guillem Cucurull, Arantxa Casanova, Adriana Romero, Pietro Liò, and Yoshua Bengio. Graph attention networks. In *Proceedings of the 6th International Conference on Learning Representations (ICLR)*, 2018.
- Oriol Vinyals, Meire Fortunato, and Navdeep Jaitly. Pointer networks. In *Advances in Neural Information Processing Systems*, volume 28, pages 2692–2700, 2015.
- Jiangjiang Wang and Yun Fong Lin. Reinforcement learning for spare parts inventory management with a deep q-network. *arXiv preprint arXiv:2103.14110*, 2021.
- Xianliang Yang, Zhihao Liu, Wei Jiang, Chuheng Zhang, Li Zhao, Lei Song, and Jiang Bian. A versatile multi-agent reinforcement learning benchmark for inventory management. *arXiv preprint arXiv:2306.07542*, 2023.
- Vinicius Zambaldi, David Raposo, Adam Santoro, Victor Bapst, Yujia Li, Igor Babuschkin, Karl Tuyls, David Reichert, Timothy Lillicrap, Edward Lockhart, Murray Shanahan, Victoria Langston, Razvan Pascanu, Matthew Botvinick, Oriol Vinyals, and Peter Battaglia. Deep reinforcement learning with relational inductive biases. In *International Conference on Learning Representations*, 2019. URL <https://openreview.net/forum?id=HkxaFoC9KQ>.
- Paul H. Zipkin. *Foundations of Inventory Management*. McGraw-Hill, 2000.